The Egyptian Journal of Radiology and Nuclear Medicine (2015) 46, 1105–1110

Egyptian Society of Radiology and Nuclear Medicine

The Egyptian Journal of Radiology and Nuclear Medicine

www.elsevier.com/locate/ejrnm
www.sciencedirect.com

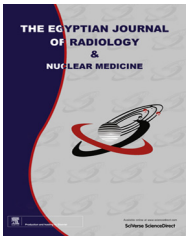

REVIEW

Segmentation of Glioblastoma Multiforme from MR Images – A comprehensive review

V.R. Simi [a], **Justin Joseph** [b,*]

[a] *Dept. of Computer Science & Engg., Arunachala College of Engg. for Women, Tamil Nadu 629 203, India*
[b] *School of Electronics, St. Joseph's College of Engg. & Tech., Kerala 686 571, India*

Received 2 February 2015; accepted 1 August 2015
Available online 21 August 2015

KEYWORDS

Glioblastoma Multiforme;
Necrosis;
Perifocal edema;
Segmentation

Abstract Delineation of active tumor region and perifocal edema from Magnetic Resonance (MR) images of Glioblastoma Multiforme (GBM) is difficult as GBM is highly infiltrating and non-enhancing on imagery. The segmentation becomes challenging when the tissue classes in the perifocal region, such as White Matter (WM) and edema, similarly, necrosis and Gray Matter (GM) are homogenous in intensity and texture. Precise delineation of GBM-focus and perifocal edema is mandatory for surgical and Radio Therapy (RT) planning and for the evaluation of tumor progress and efficiency of treatment. This article is a comprehensive review on techniques used for the segmentation of GBM from MR images.

Contents

1. Introduction

Glioma is an intracranial neoplasm, deformed from glial cells. According to the American Cancer Society (ACS) directives, glioma can be primarily classified into ependymoma and astrocytoma. Glioblastoma Multiforme is the most common astrocytoma which is a high-grade glioma comprising grade III and

* Corresponding author at: Department of Instrumentation, St. Joseph's College of Engg. & Technology, Pala, Kottayam 686 579, Kerala, India. Mobile: +91 8547783968, +91 4822 239301, +91 4822 239302; fax: +91 4822 239307.
E-mail addresses: simijijeesh@gmail.com (V.R. Simi), josephjusti@gmail.com (J. Joseph).

Peer review under responsibility of Egyptian Society of Radiology and Nuclear Medicine.

http://dx.doi.org/10.1016/j.ejrnm.2015.08.001

grade IV of WHO grading. GBMs are usually present with extensive areas of necrosis, pseudo-palisading, vasogenic edema and infiltrative microscopic disease. Precise segmentation of active tumor region and perifocal edema extension from MRI is essential for planning stereotactic biopsy, GBM resection and Radio Therapy (RT). Volumetric estimation of GBM is vital in studying tumor progress and treatment efficiency. But this proliferative lesion is undifferentiated and non-enhancing on MR images.

None of the imaging modalities including Computed Tomography (CT) and MRI and even powerful MR sequences like spectroscopic perfusion studies offer sufficient image quality to differentiate GBM and its perifocal edema. T1-weighted images without contrast are less sensitive to GBM and edema. Even in heavily T2-weighted sequences, the GBM focus is not well separated from surrounding edema. Spectroscopic perfusion diffusion MRI studies fail to define the GBM extent from perifocal vasogenic edema, as tracking the exact point of spectral changes, corresponding to the tumor boundary, is difficult. Preoperative biopsy proven axial plane images of non-enhancing and highly infiltrating GBM of different MR series are depicted in Fig. 1.

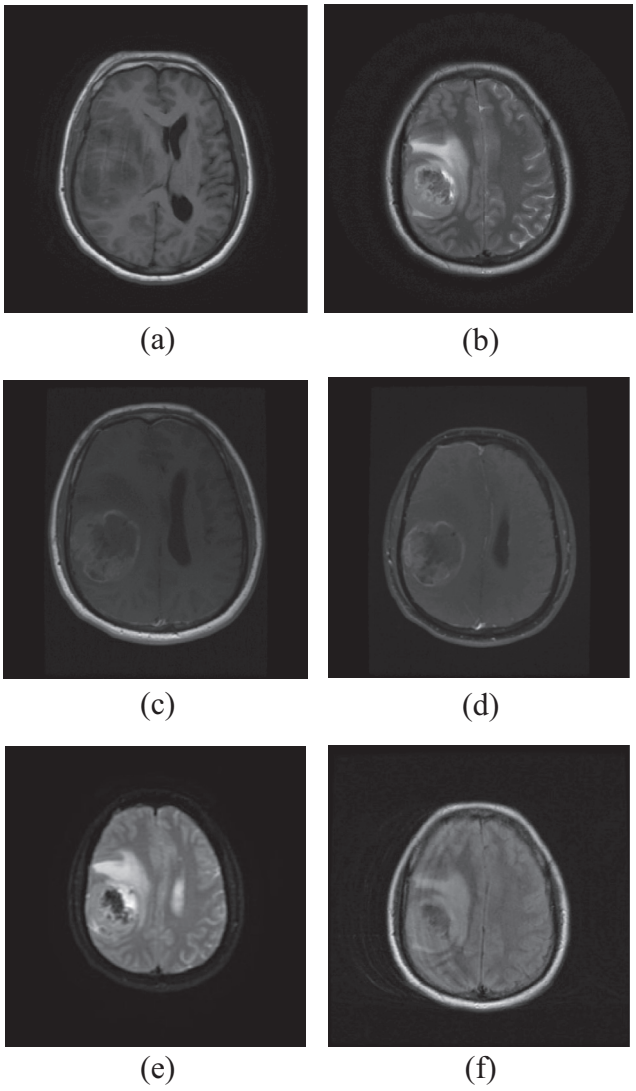

Fig. 1 Preoperative biopsy proven axial plane MR images of non-enhancing and highly infiltrating GBM of different sequences (a) T2 weighted (b) T1 weighted (c) spectroscopic (d) T1 contrast (e) Diffusion Weighted (f) FLAIR. (Image Courtesy: Hind Labs, Govt. Medical College, Kottayam, Kerala.)

Automated and computerized segmentation approaches for the delineation and quantification of GBM, or in general, any neoplasm, are meant to remove the subjectivity, inherent in time intense manual outlining. In addition to the poor tissue contrast on MRI, subregions in the active and perifocal areas of GBM exhibit homogenous gray levels. This intensity overlap happens between necrosis and Gray Matter (GM) and similarly, between White Matter (WM) and peritumoral edema. In sagittal and coronal planes the scenario become still complex. Hence, the segmentation of highly infiltrating and non-enhancing GBM from MR images is difficult than well enhanced lesions. This article presents a comprehensive review on the segmentation schemes experimented on GBM-edema complex.

2. Segmentation schemes for GBM

Elnakib et al. (1) identified the segmentation schemes popularly employed on medical images as rule-based, statistical, atlas-based and deformable model based techniques. Global as well as adaptive thresholding, region growing and region split-and-merge techniques were grouped under the rule based schemes. Atlas based method was broadly categorized as single and multi-atlas-based segmentation. Deformable models include parametric deformable models, geometric level-set based deformable models etc. Exclusive focus of this article is on segmentation of GBM rather than a broad perspective of segmentation of medical images.

Egger et al. (2) provided a variability analysis among the segmentation done by different physicians. Four physicians segmented GBMs in ten patients, once using the region-growing based Grow-Cut segmentation module of Slicer, and once by drawing boundaries completely manually, slice-by-slice. The time required for Grow-Cut segmentation was on an average 61% of the time required for the pure manual segmentation. A comparison of Slicer-based segmentation with manual slice-by-slice segmentation exhibited a Dice Similarity Coefficient (DSC) of $88.43 \pm 5.23\%$ and a Hausdorff Distance of 2.32 ± 5.23 mm.

Computerized volumetry and manual segmentation were compared in the retrospective study (3) on MR images of patients with native glioblastoma with the imaging performed at 24–48 h following resection and 2–4 months postoperatively. 1D and 2D measurements were performed by two neuro-radiologists. Computer-assisted volumetry was performed through a combination of region-based active contours and a level set approach. Tumor response was assessed by using established 1D, 2D, and volumetric standards. Twenty-nine patients were analyzed. Discrepancy in disease status between 1D and 2D compared with computer-assisted volumetry was 10.3% (3/29) and 17.2% (5/29), respectively. The mean time for segmentation between manual and computer-assisted volumetry techniques was 9.7 min and less than one minute, respectively. Inter-observer correlation was highest for volumetric measurements (0.995; 95% Concordance Index (CI), 0.990–0.997) compared with 1D (0.826; 95% CI, 0.695–0.904) and 2D (0.905; 95% CI, 0.828–0.948) measurements.

The effectiveness of knowledge-guided [KG] and supervised k-Nearest Neighbors [kNN] segmentation for delineating the GTV from MR images of GBM was evaluated in Mazzara et al's study (4). The average accuracy of the kNN was 56% +/− 6% for 11 cases, whereas that of the KG was 52% +/− 7% for 7 of the 11 cases, compared with the physician's contours. The literature observed that kNN and KG are least accurate in contouring Gross Tumor Volume (GTV) in non-enhancing GBMs. A modified kNN tissue classification was applied to 59 longitudinal MR data sets of thirteen patients with recurrent GBM, undergoing bevacizumab (anti-angiogenic) therapy, in Liberman et al's study (5). Changes in the estimated volume of the enhancing tumor were compared with Macdonald's criteria and manual volumetric measurements. The suspected edema was further sub-classified into peri- and non-peri-tumoral edema, using both the KNN method and Expectation Maximization (EM). The EM defined five clusters, three of which were related to the peri-tumoral edema and one to the non-peri-tumoral edema. The overlap fraction between the kNN and manual delineation of the enhancing tumor tissue was 0.69.

MR sequences were manipulated with a framework which combines Knowledge-Based (KB) techniques with multispectral analysis, in the literature (6). Primary segmentation from an unsupervised Fuzzy C Means (FCM) along with the cluster centers of each class was fed to a rule-based expert system. Multispectral histogram analysis was used to isolate the GBM from the rest of the intracranial region, with the region analysis used in performing the final tumor labeling. Knowledge-based Fuzzy C-Means (FCM) was used in Emblem et al's study (7) to estimate glioma volumes from Dynamic Susceptibility Contrast (DSC) images.

Xue et al. (8) applied an initial knowledge-based fuzzy clustering followed by the Support Vector Machine (SVM) active learning approach to segment GBM from multi-modal MR images. The former algorithm was employed to roughly distinguish WM, GM, CSF, T2-hyperintense regions, necrosis and enhanced pathology, and the latter to refine this rough segmentation. A hybrid of FCM and region growing was employed in Kazerooni et al's study (9) to characterize the regions of active tumor, necrosis and peri-tumoral vasogenic edema from Diffusion Weighted (DWI), Proton Weighted (PWI) and T2-Weighted MR sequences. A fuzzy formulation of region growing with an automatic initialization of the seed points through a Region Growing-FCM hybrid was introduced in (10). Fuzzy connectedness framework was adapted in Liu et al's study (11) for the segmentation of enhancing active tumor, non-enhancing tumor, edema and tumor-edema complex from FLAIR, T1, and T1 Gd contrast MR sequences. A confidence map averaging (CMA) of three individual strategies, fuzzy connectedness, Grow Cut and voxel classification on T1 post-contrast isotropic MR images was demonstrated in (12). FCM and Otzu's threshold were the choice for the evaluation of the extent of glioblastoma resection in Cordova et al's study (13). Phillips et al. (14) also claimed unsupervised FCM to be a viable solution for GBM separation. A multilevel front propagation algorithm which is an extension of level set technique was used for the extraction of glioma in Droske et al's study (15).

An 'Assisted Follow-up In Neuro Imaging of Therapeutic Intervention (FINITI) pipeline' for segmenting MR images by combining voxel-based and deformable model based schemes was proposed in Zhu et al's study (16). In the first stage, the voxel-based segmentation using the FSL FAST was performed automatically for initial tumor segmentation from T1-weighted images. The T2-weighted images were also automatically segmented and combined with the T1 segmentation results. Then, a level-set-based segmentation was used to refine the segmentation results with minimal manual input by embedding the major functions of itk-SNAP. These tools were integrated into one pipeline with a single Graphical User Interface (GUI). The AFINITI pipeline was validated by applying the software to 26 clinical GBM cases by comparing with the manual segmentation. Over 26 test images, the mean Jaccard Index (JI) was 54.42%. The maximum JI obtained was 80.70% and in some cases the segmentation was worst with JI 21.3%.

Unkelbach et al. (17) investigated the use of a phenomenological tumor growth model for treatment planning. The model was based on the Fisher Kolmogorov equation, which formalizes the growth characteristics of glioma and estimates the spatial distribution of tumor cells in normal appearing regions of the brain. The target volume for radiotherapy planning was defined as an isoline of the simulated tumor cell density.

A generative approach for simultaneous registration of a probabilistic atlas of a healthy population to brain MR images exhibiting astrocytoma and characterizing the images into anomaly as well as healthy tissue labels was investigated in the literature (18). The method was based on the Expectation Maximization (EM) algorithm that incorporates a glioma growth model for atlas seeding. The modified atlas was registered into the patient space and utilized for estimating the posterior probabilities of various tissue labels. EM iteratively refines the estimates of the posterior probabilities of tissue labels, the deformation field and the tumor growth model parameters.

Weizman et al. (19) introduced an automatic method for isolating Optic Pathway Gliomas (OPGs). The approach begins with the automatic localization of the OPG and its nodule with an anatomical tumor atlas followed by a binary voxel classification with a probabilistic tissue model, whose parameters were estimated from MR images. The method effectively incorporated prior location, shape, and intensity information to accurately identify the sharp OPG boundaries.

EM algorithm was employed in Simon et al's study (20) to delineate the areas of high and low proliferation in heterogeneous gliomas from predefined manual GTVs on 2D DWI slices. The EM was initialized manually from the contoured ROIs. High and low proliferation areas, identified from the spatial distribution of Apparent Diffusion Coefficient (ADC) had no histopathological evidence. Moreover, EM is prone to partial volume error.

A super-pixel-based graph spectral clustering method for GBM segmentation from multimodal MR images including T2 weighted (T2), T1 weighted, T1 contrast (T1+C) and FLAIR was introduced in Su et al's study (21). Initially, MR images were segmented into a number of compact and homogeneous super pixels using local k-means with weighted distance. Then, by considering the brain as a graph of super-pixels (defining nodes as super-pixels and links as similarity among super-pixels), segmentation was achieved using spectral clustering of the super-pixel network. Normalized Cut (N-Cut) can yield good results only when the shape of GBM is compact

and regular. Furthermore N-cuts need to solve a generalized Eigen vector problem when the image size is large, increasing the computational burden.

In the Literature (22), k-means algorithm was the choice for soft tissue differentiation and based on intensity feature, and Hierarchical Self-Organizing Map (HSOM) was applied for identifying the malignant zone.

A method for automatic segmentation of heterogeneous image data which bridges the gap between bottom-up affinity-based segmentation and top-down generative model based approaches was discussed in Corso et al's study (23). A Bayesian formulation was used for incorporating soft model assignments into the calculation of affinities. The resulting model-aware affinities were integrated into the segmentation by weighted aggregation algorithm, and the technique was applied to segment GBM-focus and perifocal edema in multi-channel MR volumes.

A decision forest that uses context-aware spatial features was used to differentiate necrosis and vasogenic edema in the perifocal region of GBM in (24). This framework integrated a generative model of tissue appearance, from the probabilities obtained through tissue-specific Gaussian mixture models, as additional input to the forest.

In current practice, radiotherapy planning is primarily based upon T2 FLAIR MRI despite its known lack of specificity in the detection of tumor infiltration. While hyper intensity on T2 FLAIR is widely considered to represent infiltrative tumor, it may also be caused by the presence of vasogenic edema. Le et al. (25) studied a data set of 17 GBM patients treated with anti-angiogenic therapy for which a fast decrease of T2 FLAIR hyper signal was observed, which indicates the resolution of edema. The literature investigated whether multimodal MRI acquisitions including DTI can distinguish between edema and tumor infiltration prior to therapy. Up to 75% of the extent of the edema was characterized using the morphological information from the contrast enhanced T1 image using a random forest classifier. The information from different imaging modalities did not significantly improve the classification.

A discriminative random decision forest framework that offers a voxel-wise probabilistic characterization of the Volume of Interest (VOI) was used in Geremia et al's study (26) to segment GBM from 3D MR images of T1, T1+C, T2 and FLAIR sequences.

A scheme for spherical objects that creates a directed 3D graph was used to segment GBM in Egger et al's study (27). Thereafter, the minimal cost closed set on the graph was computed via a polynomial time s–t cut, creating an optimal segmentation of the GBM nodule. Author demonstrated the flexibility that user can improve the results by specifying an arbitrary number of additional seed points to support the algorithm with gray level information and geometrical constraints. The method showed an average DSC of 77.72%.

Pedoia et al's study (28) was structured over the belief that sagittal symmetry of normal brain is disturbed by the pathology. In this literature, clustering method based on energy minimization through Graph-Cut was applied on the volume computed as a difference between the left hemisphere and the right hemisphere mirrored across the symmetry plane. This differential analysis involves the loss of the knowledge of the tumor side. The assumption that pathologies are generally not symmetrically spaced in both hemispheres, used to detect the anomaly may not be satisfied.

Hori et al. (29) discussed a semi-automated approach in which a sphere VOI including the GBM was selected manually in the 3D image and the sphere VOI was transformed to 2D space by a spiral-scanning technique. An Active Contour Model (ACM) was employed to delineate an optimal outline of the GBM in the transformed 2D image. After inverse transform of the optimal outline to the 3D space, a morphological filter was applied to smooth the boundary of the 3D segmented region. JI and the True Segmentation Coefficient (TSC) of 74.2+/−9.8% and 84.1+/−7.1%, respectively were reported. Zukic et al. (30) discussed another semi-automatic approach based on balloon inflation forces, experimented over Gadolinium contrast MR images. Resmi and Thomas (31) made use of morphological filtering techniques to delineate the neoplasm from well enhanced specimen images of low grade glioma. A comparative evaluation of the accuracy of different segmentation schemes on GBM-edema complex is furnished in Table 1. In the entire cases manual contour is the ground truth. For the literature making use of exactly same segmentation scheme, overall performance is evaluated by collectively considering the individual observations.

3. Discussions

Model based probabilistic segmentation frameworks like EM usually assume and fit the probability distribution of the intensities to some model, most often Gaussian or normal. In fact, the pathology or hyperplasic lesions modifies this underlying distribution. EM segmentation strongly depends on the parameter initialization. There is no generally accepted method for parameter initialization in EM. Learning a Gaussian mixture by EM can be difficult because the true number of mixing components is usually unknown and the algorithm can get trapped in one of the many local maxima

Table 1 The accuracy of different segmentation schemes on GBM-edema complex.

Si No	Segmentation approach	Dice similarity index (%)
1	Region-growing based Grow-Cut	88.43 ± 5.23
2	Knowledge-guided	52 ± 7
3	Supervised k-Nearest Neighbors	56 ± 6
4	Knowledge-based Fuzzy C-Means	83.4 ± 2
5	Region Growing-FCM hybrid	96.38 ± 7.16
6	Fuzzy connectedness framework	95.8 ± 3
7	Otsu's threshold	94.2 ± 2.8
8	SVM active learning	85.7 ± 3.8
9	Hybrid of voxel-based and deformable model based schemes	54.42 ± 26
10	Random forest classifier	75 ± 2
11	Polynomial time s–t cut based directed graph	77.72 ± 1.2
12	Active Contour Model	84.1 ± 7.1
13	Semi-automatic approach based on balloon inflation forces	80.46 ± 7.42
14	GMM based decision forest	80 ± 10.2
15	Super-pixel-based graph spectral clustering	83 ± 7
16	Expectation Maximization	95.6 ± 4.7

of the likelihood function. Efficient initialization is an important preliminary process for the future convergence of the algorithm to the best local maximum of the likelihood function.

In EM, the initialization is commonly chosen randomly and as a consequence results are not reproducible, do not take advantage of inherent patterns in the data or may be initialized on outliers. Random initialization is not data driven and is far from optimal and does not eliminate the problem of converging to local maxima. In addition, the segmentation results returned by the EM algorithm will be different, any time the algorithm is executed, say the reproducibility of segmentation results is poor.

Similar to EM, k-means and FCM also need prior knowledge of number of tissue classes comprised in the image and mean intensity of each tissue class. In addition to mean intensity of tissue classes EM requires tissue class variance and tissue fraction. As EM, k-means and FCM also may get trapped themselves in the local maxima. FCM may produce empty clusters and fails in images, heavily corrupted by noise. EM, FCM and k-means need strong pre-processing including contrast enhancement and restoration. Semi-automated methods such as ACM and level sets need an initial contour of the ROI, usually drawn manually and they are computationally intense too.

In contrast to unsupervised segmentation, the success of supervised ones depends on manually defined training data. Estimated volume of glioma may be erroneous if initial knowledge based operations are improper. In areas with heterogeneous MR image intensity or indistinct borders between tissue types, even the manual contouring is difficult and uncertain. Segmentation techniques based on the pixel intensities are inherently prone to partial volume effect and intra/interslice intensity variations due to inhomogeneities in the MR imaging field.

Methods like N-Cut can yield good results only when the shape of GBM is compact and regular. Often, GBM appears quite irregular. Furthermore N-cuts need to solve a generalized Eigen vector problem when the image size is large, increasing the computational burden. The technique for detecting the GBM from the sagittal symmetry is only applicable in axial plane images. The assumption that pathologies are generally not symmetrically spaced in both hemispheres, used to detect the anomaly may not be satisfied.

4. Conclusion

The techniques employed for the segmentation of GBM from MR images have been comprehensively reviewed in this article. The segmentation schemes discussed in the literature includes primarily, FCM, EM, k-means, ACM, level set, graph cut etc. The average accuracy of the kNN was reported to be 56% +/− 6% whereas that of the KG was 52% +/− 7%, compared with the physician's contours. The overlap fraction between the kNN and manual delineation of the enhancing tumor was 69% while performing the differentiation on a pre-contoured Clinical Target Volume (CTV). AFINITI pipeline that combined voxel-based and level set reported a mean JI of 54.42%, compared with the manual segmentation. The maximum JI obtained was 80.70% and in some cases the segmentation was worst with JI 21.3%. The semi-automated method based on polynomial time s–t cut, exhibited an average DSC of 77.72%. For another semi-automated method based on ACM, JI and the TSC of 74.2+/−9.8% and 84.1 +/−7.1%, respectively were reported. Semi-automatic approach based on balloon inflation forces obtained a DSC of 80.46+/−7.42. Localization of the OPG by employing anatomical tumor atlas and binary voxel classification with probabilistic tissue model exhibited mean volume overlap difference of 30.6%.

Conflict of interest

The authors declare that there are no conflicts of interest.

References

(1) Elnakib A, Gimel'farb G, Suri JS, El-Baz A. Medical image segmentation: a brief survey, handbook of multi-modality state-of-the-art medical image segmentation and registration methodologies, 2. New York: Springer-Verlag; 2011 [Chapter 1], 1–39, ISBN: 978-1-4419-8203-2.

(2) Egger J, Kapur T, Fedorov A, Pieper S, Miller JV, Veeraraghavan H, et al. GBM volumetry using the 3D slicer medical image computing platform. Sci Rep 2013. http://dx.doi.org/10.1038/srep01364, PMCID: PMC3586703.

(3) Chow DS, Qi J, Guo X, Miloushev VZ, Iwamoto FM, Bruce JN, et al. Semi automated volumetric measurement on post contrast MR imaging for analysis of recurrent and residual disease in glioblastoma multiforme. Am J Neuroradiol 2014;35:498–503. http://dx.doi.org/10.3174/ajnr.A3724, Epub 2013 Aug 29.

(4) Mazzara GP, Velthuizen RP, Pearlman JL, Greenberg HM, Wagner H. Brain tumor target volume determination for radiation treatment planning through automated MRI segmentation. Int J Radiat Oncol Biophys 2004;59:300–12.

(5) Liberman G, Louzoun Y, Aizenstein O, Blumenthal DT, Bokstein F, Palmon M, et al. Automatic multi-modal MR tissue classification for the assessment of response to bevacizumab in patients with glioblastoma. Eur J Radiol 2013;82:87–94.

(6) Clark MC, Hall LO, Goldgof DB, Velthuizen R, Murtagh FR, Silbiger MS. Automatic tumor segmentation using knowledge-based techniques. IEEE Trans Med Imag 1998;17:187–201.

(7) Emblem KE, Nedregaard B, Hald JK, Nome T, Due-Tonnessen P, Bjornerud A. Automatic glioma characterization from dynamic susceptibility contrast imaging: brain tumor segmentation using knowledge-based fuzzy clustering. J Mag Reson Imag 2009. http://dx.doi.org/10.1002/jmri.21815.

(8) Xue Z, Chi L, Yang J, Wong ST. Support vector machine (SVM) active learning for automated Glioblastoma segmentation. 9th IEEE International Symposium on Biomedical Imaging (ISBI). 2012, pp. 598–601, doi: 10.1109/ISBI.2012.6235619.

(9) Kazerooni AF, Mohseni M, Rad HS. Accurate segmentation of tumorous regions in high-grade glioma employing a multi-parametric (ADC/PWI/T2-W) image fusion approach. Frontiers Biomed Technol 2014.

(10) Veloz A, Chabert S, Salas R, Orellana A, Vielma J. Fuzzy spatial growing for Glioblastoma Multiforme segmentation on brain Magnetic Resonance Imaging. Prog Pattern Recog Image Anal Appl 2007;4756:861–70.

(11) Liu J, Udupa JK, Odhner D, Hackney D, Moonis G. A system for brain tumor volume estimation via MR imaging and fuzzy connectedness. Comput Med Imag Graph 2005;29:21–34.

(12) Huo J, Van Rikxoort EM, Okada K, Kim HJ, Pope W. Confidence-based ensemble for GBM brain tumor segmentation. SPIE 7962 Med Imag 2011. http://dx.doi.org/10.1117/12.877913.

(13) Cordova JS, Schreibmann E, Hadjipanayis CG, Guo Y, Hui-Kuo G, Shim SH, et al. Quantitative tumor segmentation for evaluation of extent of glioblastoma resection to facilitate multisite clinical trials. Trans Oncol 2014;7:40–7.
(14) Phillips WE, Velthuizen RP, Phuphanich S, Hall LO, Clarke LP, Silbiger ML. Application of fuzzy c-means segmentation technique for tissue differentiation in MR images of a hemorrhagic glioblastoma multiforme. Mag Reson Imag 1995;13:277–90.
(15) Droske M, Meyer B, Rumpf M, Schaller K. An adaptive level set method for medical image segmentation. Inform Process Med Imag Lect Notes Comput Sci 2001;2082:416–22.
(16) Zhu Y, Young GS, Xue Z, Huang RY, You H, Setayesh H, et al. Semi-automatic segmentation software for quantitative clinical brain glioblastoma evaluation. Acad Radiol 2012;19:977–85. http://dx.doi.org/10.1016/j.acra.2012.03.026, Epub 2012 May 15.
(17) Unkelbach J, Menze BH, Konukoglu E, Dittmann F, Le M, Ayache N, et al. Radiotherapy planning for glioblastoma based on a tumor growth model, improving target volume delineation. Phys Med Biol 2014;5:747–70. http://dx.doi.org/10.1088/0031-9155/59/3/747, Epub 2014 Jan 20.
(18) Gooya A, Pohl KM, Bilello M, Cirillo L, Biros G, Melhem ER, et al. GLISTR: glioma image segmentation and registration. IEEE Trans Med Imag 2012;31:1941–54. http://dx.doi.org/10.1109/TMI.2012.2210558.
(19) Weizman L, Joskowicz L, Ben-Sira L, Precel R and Ben-Bashat D. Automatic segmentation of optic pathway gliomas in MRI. IEEE international conference on biomedical imaging: from nano to macro; 2010. p. 920–3.
(20) Simon D, Fritzsche KH, Thieke C, Klein J, Parzer P, Weber MA, et al. Diffusion-weighted imaging-based probabilistic segmentation of high- and low-proliferative areas in high-grade gliomas. J Cancer Imag 2012;5:89–99. http://dx.doi.org/10.1102/1470-7330.2012.0010.
(21) Su P, Yang J, Li H, Chi L, Xue Z, Wong ST. Superpixel-based segmentation of glioblastoma multiforme from multimodal MR images. Multimodal Brain Image Anal Lect Notes Comput Sci 2013;8159:74–83.
(22) Shreeshayana R, Udayashankara V. Glioma Multiforme brain tumor segmentation using soft computing techniques with integrated radiology study maker. International Conference on Electronics and Communication Engineering. Bengaluru; 2013, ISBN: 978-93-83060-04-7.
(23) Corso JJ, Sharon E, Dube S, El-Saden S, Sinha U, Yuille A. Efficient multilevel brain tumor segmentation with integrated bayesian model classification. IEEE Trans Med Imag 2008;27 (629):640. http://dx.doi.org/10.1109/TMI.2007.912817.
(24) Zikic D, Glocker B, Konukoglu E, Criminisi A, Demiralp C, Shotton J, Thomas OM, Das T, Jena R, Price SJ. Decision forests for tissue-specific segmentation of high-grade gliomas in multi-channel MR. Medical Image Computing and Computer-Assisted Intervention – MICCAI. 2012; 7512:369–376.
(25) Le M, Delingette H, Cramer JK, Gerstner E, Shih H, Batchelor T, Unkelbachand J, Ayache N. Multimodal analysis of vasogenic edema in glioblastoma patients for radiotherapy planning. The MIDAS Journal – Image-Guided Adaptive Radiation Therapy (IGART). <http://hdl.handle.net/10380/3500>.
(26) Geremia E, Menze B, Ayache N. Spatial decision forests for glioma segmentation in multi-channel MR images. MICCAI BRATS (Brain Tumor Segmentation Challenge) Nice, France; 2012
(27) Egger J, Bauer MHA, Kuhnt D, Kappus C, Carl B, Freisleben B and Nimsky C. A flexible semi-automatic approach for glioblastoma multiforme segmentation biosignal 2010, Berlin, Germany; 2010.
(28) Pedoia V, Binaghi E, Balbi S, Benedictis AD, Monti E, Minotto R. Glial brain tumor detection by using symmetry analysis. SPIE 8314 Med Imag 2012. http://dx.doi.org/10.1117/12.910172.
(29) Hori D, Katsuragawa S, Murakami R, Hirai T. Semi-automated segmentation of a glioblastoma multiforme on brain MR images for radiotherapy planning. Nihon Hoshasen Gijutsu Gakkai Zasshi 2010;66:353–62.
(30) Zukic D, Egger J, Bauer MHA, Kuhnt D, Carl B, Freisleben B, Kolb A, Nimsky C. Glioblastoma Multiforme segmentation in MRI Data with a balloon inflation approach. In: 6th Russian-Bavarian Conference on Bio-Medical Engineering; 2010.
(31) Resmi SA, Thomas T. A semi-automatic method for segmentation and 3D modelling of glioma tumors from brain MRI. J Biomed Sci Eng 2012:378–83.